International Journal of Nanomedicine

Dovepress
open access to scientific and medical research

Open Access Full Text Article

ORIGINAL RESEARCH

Vascular Pericyte-Derived Exosomes Inhibit Bone Resorption via Traf3

Mingxiang Cai[1,*], Huizhen Peng[1,*], Minyi Liu[1,*], Maohua Huang[2,3], Wen Zheng[1], Guilan Zhang[1], Wenjia Lai[1], Chufang Liao[1], Lizhao Cai[1], Dongmei Zhang[2,3], Xiangning Liu[1]

[1]The First Affiliated Hospital of Jinan University, School of Stomatology, Clinical Research Platform for Interdiscipline of Stomatology, Jinan University, Guangzhou, 510630, People's Republic of China; [2]College of Pharmacy, Jinan University, Guangzhou, 510632, People's Republic of China; [3]Guangdong Province Key Laboratory of Pharmacodynamic Constituents of Traditional Chinese Medicine and New Drugs Research, Jinan University, Guangzhou, 510632, People's Republic of China

*These authors contributed equally to this work

Correspondence: Xiangning Liu, The First Affiliated Hospital of Jinan University, School of Stomatology, Clinical Research Platform for Interdiscipline of Stomatology, Jinan University, Guangzhou, 510630, People's Republic of China, Email liuxiangning@jnu.edu.cn; Dongmei Zhang, College of Pharmacy, Jinan University, Guangzhou, 510632, People's Republic of China, Email dmzhang701@jnu.edu.cn

Purpose: Blood vessels distribute cells, oxygen, and nutrients throughout the body to support tissue growth and balance. Pericytes and endothelial cells form the inner wall of blood vessels, crucial for organ development and tissue homeostasis by producing paracrine signaling molecules. In the skeletal system, pericyte-derived vascular factors along with angiogenic factors released by bone cells regulate angiogenesis and bone formation. Although the involvement of angiogenic factors and skeletal blood vessels in bone homeostasis is relatively clear, the role of pericytes and the underlying mechanisms remain unknown. Here, our objective was to elucidate the significance of pericytes in regulating osteoclast differentiation.

Methods: We used tissue staining to detect the coverage of pericytes and osteoclasts in femoral tissues of osteoporotic mice and mice of different ages, analyzing their correlation. We developed mice with conditionally deleted pericytes, observing changes in bone mass and osteoclast activity using micro-computer tomography and tissue staining to detect the regulatory effect of pericytes on osteoclasts. Pericytes-derived exosomes (PC-EVs) were collected and co-cultured with monocytes that induce osteoclast differentiation to detect the effect of the former on the exosomes. Finally, the specific mechanism of PC-EVs regulating osteoclast differentiation was verified using RNA sequencing and Western blotting.

Results: Our study indicates a significant correlation between pericytes and age-related bone resorption. Conditional deletion of pericytes activated bone resorption and led to osteopenia in vivo. We discovered that PC-EVs inhibited the nuclear factor kappa-light-chain-enhancer of activated B cells (NF-κB) pathway, which is mediated by tumor necrosis factor receptor-associated factor 3 (Traf3), negatively regulating osteoclast development and bone resorption. Silencing Traf3 in PC-EVs canceled their inhibitory effect on osteoclast differentiation.

Conclusion: Our study provides a novel perspective into the regulatory role of pericytes on bone resorption and may provide potential strategies for developing novel anti-bone resorption therapies.

Keywords: pericytes, exosomes, bone resorption, Traf3

Introduction

Pericytes, perivascular contractile cells found in the capillaries, are key regulators of vascular stability[1,2] and tissue homeostasis.[2] Furthermore, the complex crosstalk between the bone network and vascular network is adjusted by bone cells (osteoclasts, osteoblasts, and osteocytes) and vascular cells (perivascular and endothelial cells).[3] Vascular endothelial cells secrete various angiocrine factors which affect bone cells, including osteoclasts, chondrocytes, and osteoblasts.[4] Additionally, pericyte stem cells can inhibit osteoclast differentiation,[5] while in atherosclerosis, the supernatant of pericytes cultured and collected under osteogenic conditions inhibits the differentiation of $CD14^+$ cells into

Received: 4 October 2023
Accepted: 17 November 2023
Published: 28 November 2023

Graphical Abstract

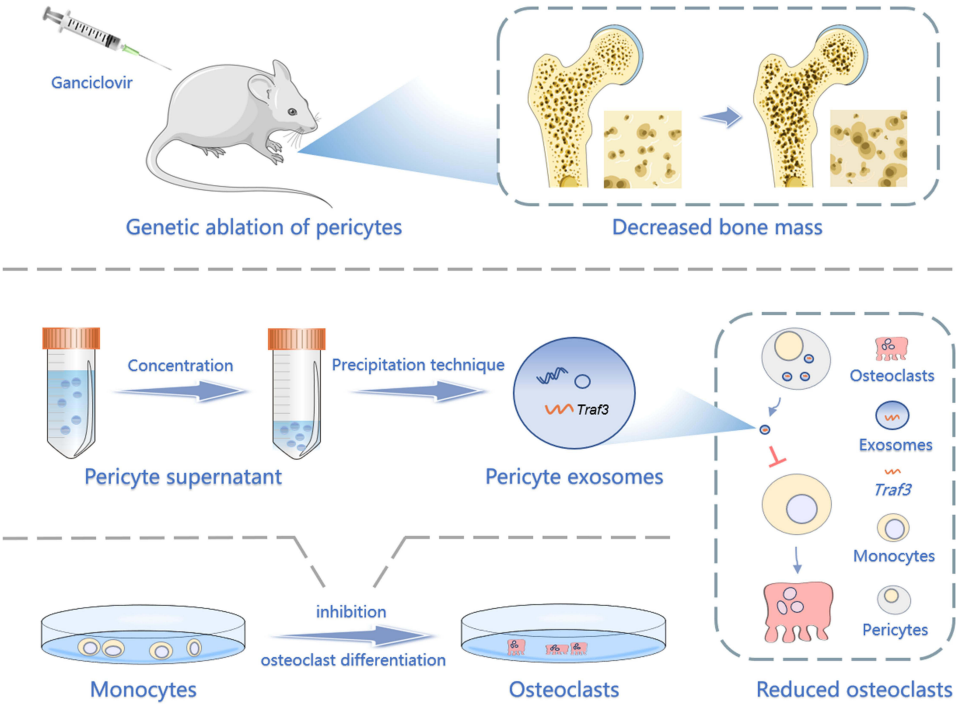

osteoclasts.[6,7] However, the function of pericytes in the development and homeostasis of the skeletal system, especially in osteoclast differentiation and bone resorption, remains unexplored.

Exosomes are nanoscale (40–160nm) extracellular vesicles with a complex composition of lipids, nucleic acids, and proteins that mediate intercellular communication.[8,9] Perivascular cells can secrete exosomes and regulate vascular function which is a critical factor in pathological conditions and diseases such as diabetes and tumors.[10,11] A close relationship between blood vessels and bone homeostasis had been reported since exosomes released by endothelial cells were found to be able to inhibit bone-marrow macrophages from differentiating into osteoclasts.[12] Furthermore, the effect of pericyte stem cell exosomes on osteoclastogenesis has also been reported.[5] However, the effect of pericyte-derived exosomes (PC-EVs) on osteoclast differentiation is unclear and needs further investigation.

Herein, our objective was to clarify the regulatory effect of pericytes on osteoclast development. Our results showed that the conditional deletion of the pericytes stimulated bone resorption and reduced bone mass. Tumor necrosis factor receptor-associated factor (Traf3) from PC-EVs inhibited osteoclast differentiation responsible for bone resorption via triggering the nuclear factor kappa-light-chain-enhancer of activated B cells (NF-κB) pathway.

Materials and Methods

Generation of Mouse Models

OVX Mouse Model

Mice were purchased from Xiaqing Biology (Guangdong, China). Female C57BL/6 mice of 12 weeks were divided into two groups (sham-operation and OVX groups, n=6 per group). Mice in the OVX group underwent ovariectomy. Breifly, mice were anesthetized with 35 mg/kg pentobarbital sodium. In a sterile environment, a 0.5 cm long incision was made at 0.5 cm to the left of the midline of the abdomen at 1 cm below the rib of the mouse. Cut the fascia and muscle, find the white adipose tissue in the lower abdomen and pull it out of the body, and find the fallopian tube and ovary in the uterus. After ligation of the fallopian tube, the ovaries and fallopian tubes were cut off. After bilateral resection, the uterus and

fat were placed in the abdomen and sutured. Femur tissues were collected three months later for immunofluorescence assay and tartrate-resistant acid phosphatase (TRAP) staining.

Mice of Different Ages

In addition, female C57BL/6 mice of 12 weeks were separated into three groups (6, 12, and 18 months, n=6 per group). The mice were housed to 6, 12 and 18 months. And the femur tissues were taken for following experiments.

NG2-tk Mice

The breeding pairs of NG2-tk mice were provided by the MD Anderson Cancer Center at the University of Texas.[13] These mice were maintained through mating wild-type (WT) FVB females with half-zygotic males and crossbreeded with BALB/c lines for more than 10 generations. Female NG2-tk mice (n = 6) and WT mice (n = 6) of 6 weeks were maintained in pathogen-free standard cages. Ganciclovir (GCV, diluted with 0.9% sodium chloride, 50 mg/kg) was administered intraperitoneally to all animals once a day for 30 days. After this treatment period, femur tissues were collected for subsequent experiments.

Hematoxylin and Eosin (H&E) Staining

The left femurs were decalcified and processed into paraffin sections. These slices underwent xylene dewaxing, a gradient ethanol series, hydration, and stained with the H&E Stain Kit (#G1120; Solarbio, Beijing, China) following the manufacturer's instructions. Subsequently, the slices were cleared in xylene for 5 minutes and then sealed with neutral resin. Images were captured using an inverted microscope (ICC50 HD, Leica, Weztlar, Germany) and Leica Application Suit software (version 4.4.0).

Micro-Computer Tomography (CT) Analysis

The right femurs of mice were examined using micro-CT (μCT 50, Scanco Medical AG, Brüttisellen, Zurich, Switzerland). The voxel size was set at 10 μm, and a total of 25 sections covering the entire femur were scanned and reconstructed to comprehensively assess changes in the bone mass of the distal femur. Additionally, specific regions, including 50 slices of cortical bone and 100 slices of trabecular bone beneath the growth plate, were rebuilt with voxel sizes of 10 μm for subsequent data analysis. A threshold of 180 was applied for image processing and data analysis, using Mimics software (version 13.0).

Immunofluorescence Assay

After deparaffinization, slices of mouse left femur were permeabilized, blocked, and incubated overnight at 4 °C with anti-NG2 and anti-endomucin antibodies (Supplementary Table S1). Then sections were washed, and the corresponding second antibody (Supplementary Table S1) was applied for an hour at 37 °C in the dark. Nuclear staining was performed with DAPI. And the fluorescence microscope (DMi8, Leica) and Leica Application Suite X software (version 3.3.3.16958) were used to acquire the images.

TRAP Staining

For TRAP staining, paraffin sections of mouse left femur tissue were dewaxed and hydrated. The TRAP Staining Kit (#387A; Sigma, Missouri, USA) was used as per the manufacturer's instructions. Briefly, slices were stained at 37 °C for 15 minutes and counterstained with methyl green dye solution (#M8020; Sigma). After rinsing with ethanol, sections were vitrified in dimethylbenzene for 5 minutes and sealed with neutral resin. For RAW264.7 cell staining, cells were induced for 5 days, fixed using 4% paraformaldehyde (4% PFA) at 4 °C for 30 minutes, and then stained with TRAP Staining Kit at 37 °C for 1 hour. Images were acquired by an inverted microscope (ICC50 HD, Leica) and Leica Application Suit software (version 4.4.0).

Cell Isolation and Cell Culture

Microvascular pericytes were isolated from mouse epiphysis as follows. Briefly, female C57BL/6 mice of 8 weeks had their femurs removed and dissected on ice. After removing muscles, fascia, and periosteum surrounding the bone tissue,

four sections of bone, including the proximal femur, femoral condyle, proximal tibial tubercle, and distal tibia were collected, while the middle 1/3 of the bone tissue was discarded. These four bone sections were longitudinally cut into 2–3 slices and cleared twice in 1% phosphate-buffered saline (PBS) for seconds. The marrow cavity wall of the thin bone slices was seeded in 24-well plates, with 3–4 pieces per well, to prevent them from floating.

The pericytes were cultured as previously described using Pericyte Medium (#1201; PM, ScienCell, Carlsbad, CA, USA) supplemented with 1% Pericyte Growth Supplement (#1252; PGS, ScienCell), 1% penicillin-streptomycin (#15140122; PS, Gibco), and 2% fetal bovine serum (#10270106; FBS, Gibco).[10] After 3 days of immobilization, the medium was replaced every other day, and cells were cultured in a 5% CO_2 atmosphere at 37 °C. Third-generation cultures were subjected to magnetic bead labeling using anti-alkaline phosphatase (ALP), anti-CD31, and anti-CD56 magnetic microbeads (Miltenyi, Shanghai, China) to remove osteoblasts and endothelial cells.[14] The labeled cells were collected through a magnetized column, eluted, and validated as pericytes through immunofluorescence assay (Supplementary Figure S2B) before subsequent investigations.

Mouse RAW264.7 macrophages (#TIB-71, from the ATCC) were sustained with Dulbecco's Modified Eagle medium including 1% PS and 10% FBS under a 5% CO2 environment at 37 °C.

Isolation and Analysis of PC-EVs

PC-EVs were isolated using previously validated protocols.[10] Thus, mouse epiphyseal pericytes from passages 3–4 were seeded into 75 cm^2 cell culture flasks and cultured until reaching 75% confluence. The medium was changed to α-MEM containing 1% PGS and 1% PS. After 24 hours, approximately 15 mL of medium was collected per flask and sterilely filtered using a 0.22 Millipore filter (#SLGV033RB; Millipore, MA, USA). PC-EVs were isolated using the cell supernatant exosome extraction kit (#UR52121; Umibio, Shanghai, China) per the manufacturer's instructions.

In brief, the pericyte culture medium was centrifuged for 10 min at 3000 g and 4 °C. Add the extraction solution to the supernatant (solution: supernatant 1: 5) and vortex. Then the mixture was incubated at 4 °C for 12 h, and centrifuged at 10, 000 × g and 4 °C for 1 h to remove the supernatant. The precipitated PC-EVs were reintroduced in 200 μL PBS and kept at −80 °C.

Quantification of PC-EVs was based on protein content, determined by the BCA Protein Assay Kit (#P0012; Beyotime, Shanghai, China).[15] The morphology of PC-EVs was examined using transmission electron microscopy (TEM).[16] Nanoparticle tracking analysis (NTA) was employed to measure PC-EV concentration (particle/mL) and particle size distribution using NanoSight NS300 (Malvern Panalytical, Malvern, UK), and the NanoSight NTA analytical software (version 2.1) was used for data analysis. The expression levels of CD9, CD63, CD81, and cadherins derived from PC-EVs were assessed by Western blotting.

RNA Transcriptome Sequencing

The RNA content of PC-EVs was analyzed via total RNA sequencing. Briefly, three different mouse pericyte supernatants were collected to obtain sufficient PC-EVs. Subsequently, PC-EVs and RNA extraction, as well as RNA sequencing were performed by Kane Biology (Guangdong, China). Kyoto Encyclopedia of Genes and Genomes (KEGG) and Gene Ontology (GO) were used to analyze differentially expressed mRNA and indicate the key genes and signaling pathways that regulate PC-EV-induced inhibition of osteoclast differentiation.

Osteoclast Differentiation from RAW264.7 Cells

For osteoclast differentiation from RAW264.7 cells, cells were seeded at a density of 2×10^4 cells/mL in 48-well plates and maintained in α-MEM medium with 10% FBS and 1% PS. Osteoclast differentiation was stimulated by adding 100 ng/mL of receptor activator of nuclear factor kappa-B ligand (RANKL) (#315-11C; Peprotech, Rocky Hill, NJ, USA).[17] To determine the optimal concentration of PC-EVs for inhibiting osteoclast differentiation, 5 μg/mL or 10 μg/mL PC-EVs, or an equivalent amount of medium, was added. To confirm the negative regulation of osteoclast differentiation by Tref3 within PC-EVs, 5 μg/mL PC-EV-(siTraf3), 5 μg/mL PC-EV-(siTraf3), 5 μg/mL PC-EVs, or the same amount of medium was added. Cells were cultured for 5 days with medium replacement every two days.

Cell Transfection

Pericytes were transfected with siRNAs for gene knockout using jet PRIME transfection reagent (#114-15; Polyplus, Illkirsh, France). This involved mixing 200 pmol siRNA with a 4 μL jet PRIME transfection reagent in a 200 μL jet PRIME buffer. After a 10-minute incubation at 37 °C, the mixture was added to the cells in a 6-well plate and incubated at 37 °C. After 48 hours, the old culture medium was removed after 6 hours. Primer sequences for siRNAs are provided in Supplementary Table S2.

Western Blotting Analysis

Cells were lysed with RIPA buffer (#BL504A; Biosharp, Guangzhou, China) containing protease inhibitor (#P1005; Beyotime). Protein concentration was determined using the BCA Protein Assay Kit (#P0012S; Beyotime), and protein expression was detected using Western blotting. The details on the primary antibodies are included in Supplementary Table S3 and the secondary antibody is listed in Supplementary Table S1. Band densities were quantified by Quantity One software (version 4.62, Bio-Rad, USA).

Quantitative Real-Time Polymerase Chain Reaction (PCR)

Total RNA isolation from pericytes was performed using TRIzol Reagent (#15596-018; Invitrogen). cDNA was synthesized using the Prime Script RT Reagent Kit with gDNA Eraser Kit (#RR047A; TaKaRa, Otsu, Japan). Quantitative real-time PCR was carried out by Hieff® qPCR SYBR® Green Master Mix (#11201ES08; Yeasen, Shanghai, China). Primer sequences are listed in Supplementary Table S3. The reaction conditions were 95 °C for 30s, 55 °C for 30s, and 40 cycles. Gene expression levels were normalized to GAPDH.

Statistical Analysis

GraphPad Prism 8.0 software was used for statistical analysis. All data are presented as mean ± standard error mean. Differences between two groups were assessed using an unpaired *t*-test, while differences among multiple groups were evaluated using one-way ANOVA and Tukey's multiple comparison test. *P*-levels < 0.05 were considered statistically significant.

Results

Pericytes Declined in Age-Related Bone Resorption and Bone Resorption Caused by Estrogen Deficiency

To explore pericyte involvement in bone resorption, we developed a mouse model of osteoporosis. Furthermore, we employed TRAP staining of the femur tissue of OVX mice to confirm the increased osteoclast activity (Figure 1A and B). Meanwhile, the femoral pericyte coverage was evaluated by immunofluorescence detection of NG2, a marker for vascular pericytes,[18,19] and endomucin, an endothelial-cell marker.[20] Compared to control mice, OVX mice exhibited a lower number of $NG2^+$ pericyte cells related to Endomucin staining in the femur. This decrease in the ratio of $NG2^+$ pericyte cells indicated that there was lower pericyte coverage associated with enhanced bone resorption (Figure 1C and D).

To further evaluate the relationship between pericyte coverage and bone resorption, we examined femur tissues from mice aged 6, 12 and 18 months. As anticipated, there was a negative correlation between osteoclast numbers and $NG2^+$ cell numbers in femurs across these age groups ($r = 0.9305$, $P < 0.0001$; Figure 1E and Supplementary Figure S1). Altogether, mice with lower pericyte coverage detected on femoral vessels showed more $TRAP^+$ osteoclasts than mice with higher pericyte coverage. These results indicated that low pericyte coverage is significantly related to enhanced bone resorption.

Genetic Ablation of Pericytes Led to Reduced Bone Mass

To further understand the impact of pericytes on skeletal tissue, we utilized transgenic NG2-tk mice that had the Ng2 promoter controlling the expression of viral thymidine kinase (tk) (Supplementary Figure S3).[13] GCV treatment in NG2-tk mice permanently inhibited DNA synthesis, which resulted in the selective reduction of $NG2^+$ perivascular cells[13]

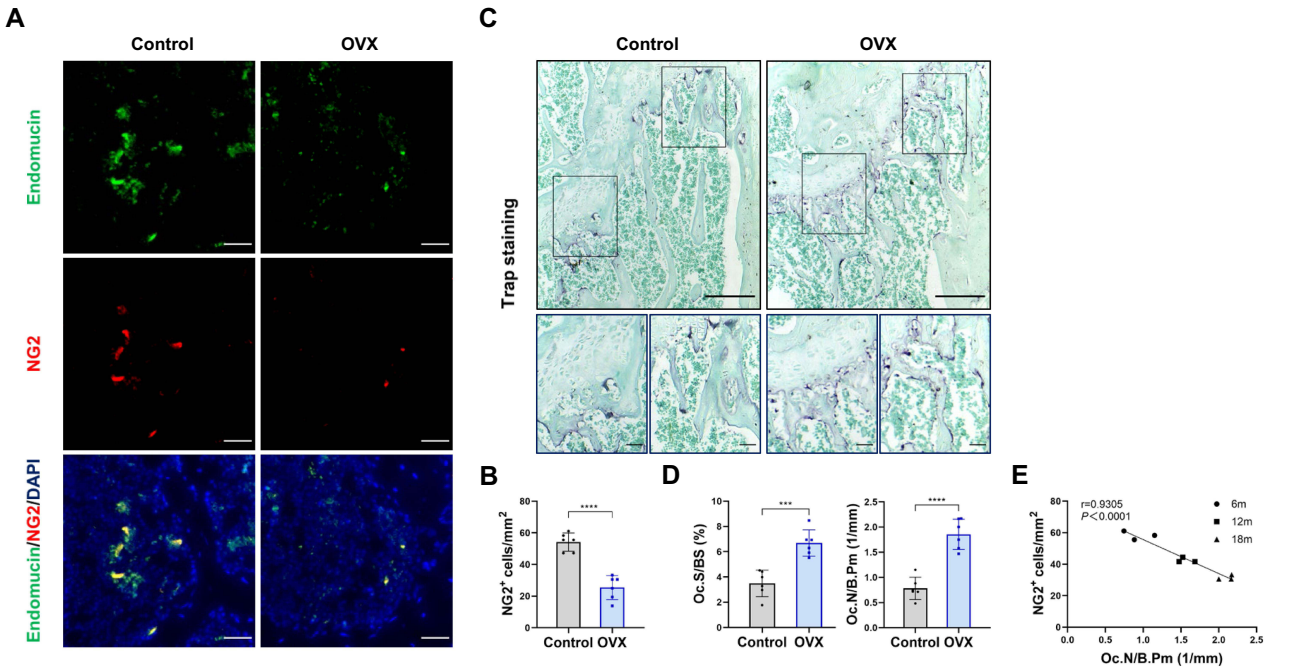

Figure 1 Pericytes declined in age-related bone resorption and bone resorption caused by estrogen deficiency (**A**) Representative immunostaining images of femurs from OVX and female WT mice. NG2$^+$ (red) pericytes, endomucin$^+$ (green) endothelial cell, and nuclear (blue) DAPI staining. Scale bar, 50 μm. (**B**) Quantification of NG2$^+$ pericyte number in subepiphyseal zone of femurs from OVX and female WT mice (n = 6). (**C**) Representative TRAP staining images of femurs from OVX and female WT mice. Scale bar, 100 μm (lower panels); 500 μm (upper panels). (**D**) Quantification of osteoclast surface per bone surface (Oc.S/BS) and osteoclast number per bone perimeter (Oc.N/B.Pm) in subepiphyseal zone of femurs from OVX and female WT mice (n = 6). (**E**) Analysis of the Pearson correlation between NG2$^+$ cell number and Oc.N/B.Pm in femurs from female wild-type mice of different ages (6, 12 and 18 months). Data are presented as the mean ± S.E.M. *P*-values < 0.05 were considered statistically significant, as follows: ***$P < 0.001$; ****$P < 0.0001$.

(Figure 2A). Quantitative micro-CT of the femurs confirmed that NG2-tk + GCV mice had lower trabecular bone mass than WT + GCV mice (Figure 2B and C). Consistently, GCV-induced loss of NG2$^+$ pericytes led to significantly less bone volume in NG2-tk + GCV animals compared to the control group, as shown by H&E staining (Figure 2D and E). These data indicate that the loss of pericytes in the skeletal system leads to a decrease in bone mass.

Genetic Ablation of Perivascular Cells Activated Bone Resorption

Reduced pericyte coverage was significantly associated with enhanced bone resorption. In this study, the efficiency of selective deletion of NG2$^+$ perivascular cells was approximately 52.82%, as evaluated through immunofluorescence detection of NG2 and endomucin (Figure 3A and B). To further understand the impact of perivascular cell deletion on osteoclast activity in skeleton, we confirmed an increased number and area of osteoclasts in the femur of NG2-tk mice through TRAP staining (Figure 3C and D). In conclusion, the GCV-induced ablation of perivascular cells resulted in enhanced bone resorption activity in the femoral tissue.

Traf3 in Exosomes Mediates the Inhibition of Osteoclast Differentiation by Pericytes

To explore how pericytes affect osteoclasts, we investigated whether perivascular cells inhibit osteoclast formation through exosomes, known mediators of intercellular communication. We isolated primary mouse epiphyseal microvascular pericytes from mouse femoral tissue and cultured them in vitro (Supplementary Figure S3A), confirming their identity through immunostaining (Supplementary Figure S3B). Subsequently, PC-EVs were extracted and analyzed. TEM revealed typical cup-shaped PC-EVs (Figure 4A).

Particle concentration, average diameter, and mode diameter were assessed using NTA, yielding values of 5.66×10^8 particles/mL, 193 nm, and 125.8 nm, respectively (Figure 4B). Western blotting confirmed that PC-EVs expressed CD9, CD81, and CD63, while cadherin, an endoplasmic reticulum marker, was absent (Figure 4C).

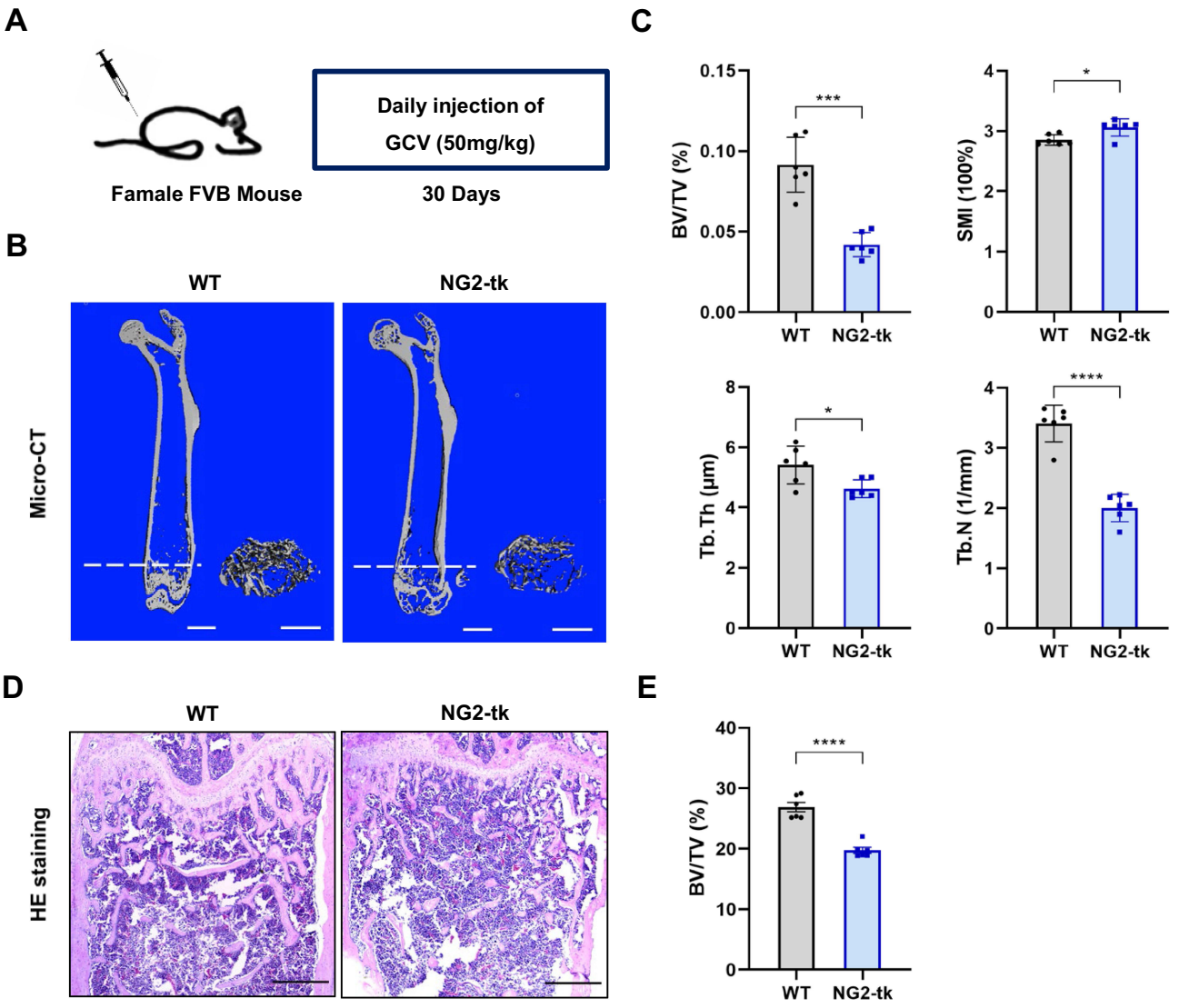

Figure 2 Genetic ablation of pericytes led to reduced bone mass (**A**) Schematic of NG2-tk mice modeling. Six-week-old female NG2-tk mice were intraperitoneally injected with GCV (50 mg/kg) once a day for 30 consecutive days in order to delete $NG2^+$ pericytes. (**B**) Representative micro-CT images displaying the three-dimensional architectures of femurs from WT mice and NG2-tk mice (after GCV treatment). Scale bar, 1mm (left panels); 500 μm (right panels). (**C**) Micro-CT analysis of BV/TV, SMI, Tb. Th, and Tb.N in femurs of WT mice and NG2-tk mice (after GCV treatment, n = 6). (**D**) Representative H&E staining images of femurs from WT mice and NG2-tk mice (after GCV treatment). Scale bar, 500 μm. (**E**) Quantification of bone volume fraction (BV/TV) in femurs from WT mice and NG2-tk mice (after GCV treatment, n = 6). Data are presented as mean ± S.E.M. *P*-values < 0.05 were considered statistically significant, as follows: **P* < 0.05; ****P* < 0.001; *****P* < 0.0001.

Subsequently, we incubated RAW264.7 cells with exosomes, observing a significant uptake of PC-EVs by RAW264.7 cells (Supplementary Figure S3C). To detect the potential direct inhibition of PC-EVs on osteoclast formation, we co-cultured RAW264.7 cells undergoing osteoclast differentiation with PC-EVs. Compared with the control group, PC-EVs had an inhibitory effect on osteoclast formation, as the Osteoclast activity was greatly reduced in the presence of PC-EVs (Figure 4D and E).

These results indicated that PC-EVs contain an osteoclast inhibitor. To investigate the potential mechanism underlying the inhibition of osteoclast formation by PC-EVs, we performed total RNA sequencing of exosomes (Figure 4F). Among the exosomal mRNAs samples from different mouse femoral pericytes, 162 were associated with osteoclast formation inhibition. Traf3, known to be involved in the non-classical NF-κB pathway, exhibited the highest expression and was chosen for further investigation (Figure 4G).

PC-EV-Traf3 Inhibits Osteoclast Differentiation Through the Non-Classical NF-κB Pathway

To elucidate the mechanism of the negative regulation of exosomal Traf3 on osteoclast differentiation, we initially silenced the *Traf3* gene using *Traf3*-specific siRNAs in mouse periosteal cells (Figure 5A). Subsequently, we cultured the

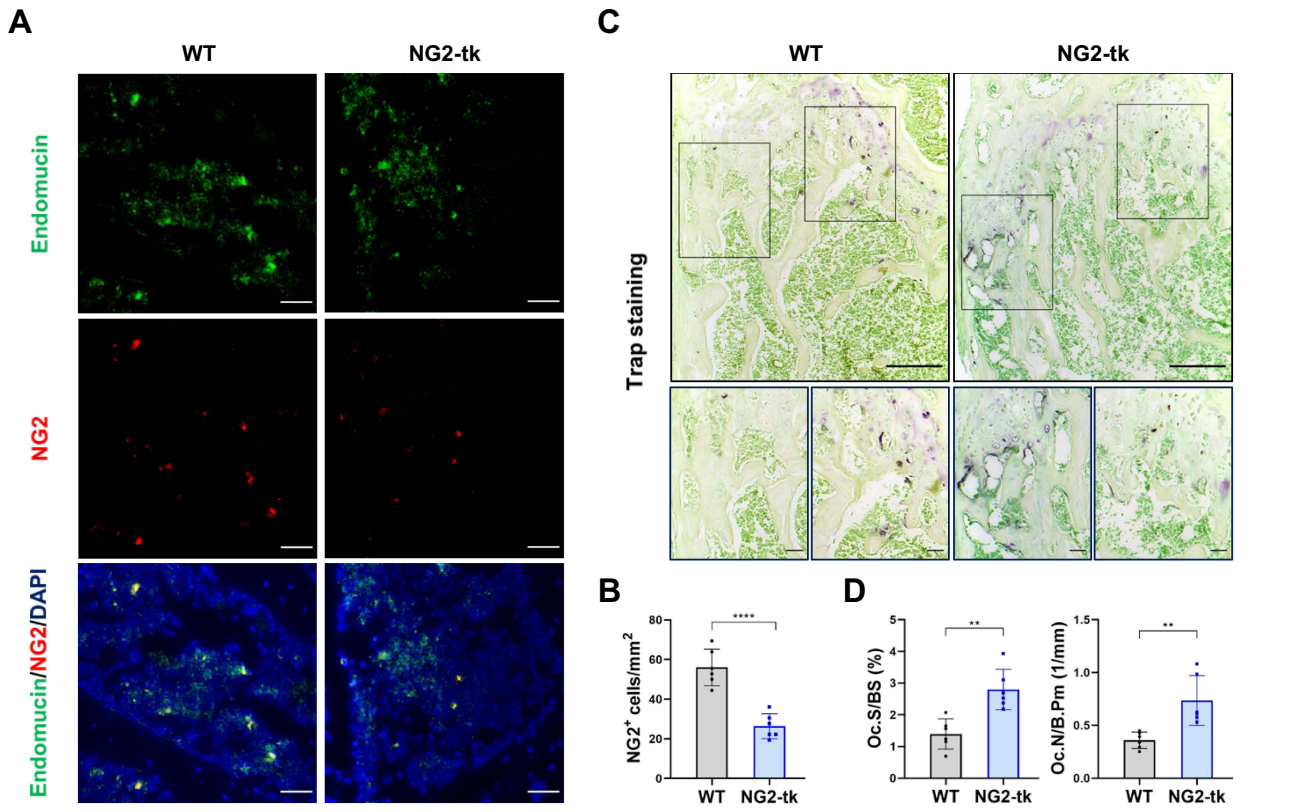

Figure 3 Genetic ablation of pericytes activated bone resorption (**A**) Representative immunostaining images of femurs from WT mice and NG2-tk mice (after GCV treatment). NG2$^+$ (red) pericytes, endomucin$^+$ (green) endothelial cell, and nuclear (blue) DAPI staining. Scale bar, 50 μm. (**B**) Quantification of NG2$^+$ pericyte number in subepiphyseal zone of femurs from WT mice and NG2-tk mice (after GCV treatment, n = 6). (**C**) Representative TRAP staining images of mouse femurs from WT mice and NG2-tk mice (after GCV treatment). Scale bar, 500 μm (upper panels); 100 μm (lower panels). (**D**) Quantification of osteoclast surface per bone surface (Oc.S/BS) and osteoclast number per bone perimeter (Oc.N/B.Pm) in subepiphyseal zone of femurs from WT mice and NG2-tk mice (after GCV treatment, n = 6). Data are presented as mean ± S.E.M. *P*-levels < 0.05 were considered statistically significant, as follows: ***P* < 0.01; *****P* < 0.0001.

pericytes with silenced *Traf3* and extracted the exosomes, generating Traf3-deficient PC-EVs (PC-EV-(siTraf3)) (Figure 5B). To investigate whether Traf3 silencing can reduce the negative regulation of PC-EVs on osteoclast formation, we conducted in vitro studies on the differentiation of RAW264.7 cells into osteoclasts. Compared to PC-EV-(siNC), PC-EV-(siTraf3) exhibited significantly reduced inhibitory effects on osteoclast differentiation, resulting in increased numbers of osteoclasts and larger osteoclast areas (Figure 5C and D).

Traf3 inhibits the sensitization of the non-classical NF-κB pathway and negatively regulates osteoclast differentiation.[21,22] However, it remains unclear whether Traf3 in PC-EVs relies on the activation of the above pathways to negatively regulate osteoclast differentiation. Osteoclast development in RAW264.7 cells was stimulated in vitro for 5 days. The results revealed that compared to PC-EV-(siNC), in PC-EV-(siTraf3)-induced osteoclasts, the protein expression levels of osteoclast markers cathepsin K (CTSK) and TRAP were significantly higher, while those of TRAF3 were lower (Figure 5E and F). In addition, compared to PC-EV-(siNC), RANKL in PC-EV-(siTraf3) treatment group could more effectively process P100 into P52, increasing the level of RElB protein (Figure 5G and H). Consistently, the P100 protein level was higher in the PC-EV-(siNC) than the PC-EV-(siTraf3) group (Figure 5G and H). The results reveal that Traf3 negatively regulates osteoclast differentiation by inhibiting the non-classical NF-κB pathway.

Discussion

Pericytes are vital vascular mural cells embedded in the basement membrane of blood vessels.[23] They are essential to vascular function.[24] The close relationship between bone system and angiogenesis is well-established. Thus, bone cells secrete various molecules to regulate angiogenesis. For instance, osteoclasts can stimulate angiogenesis by secreting

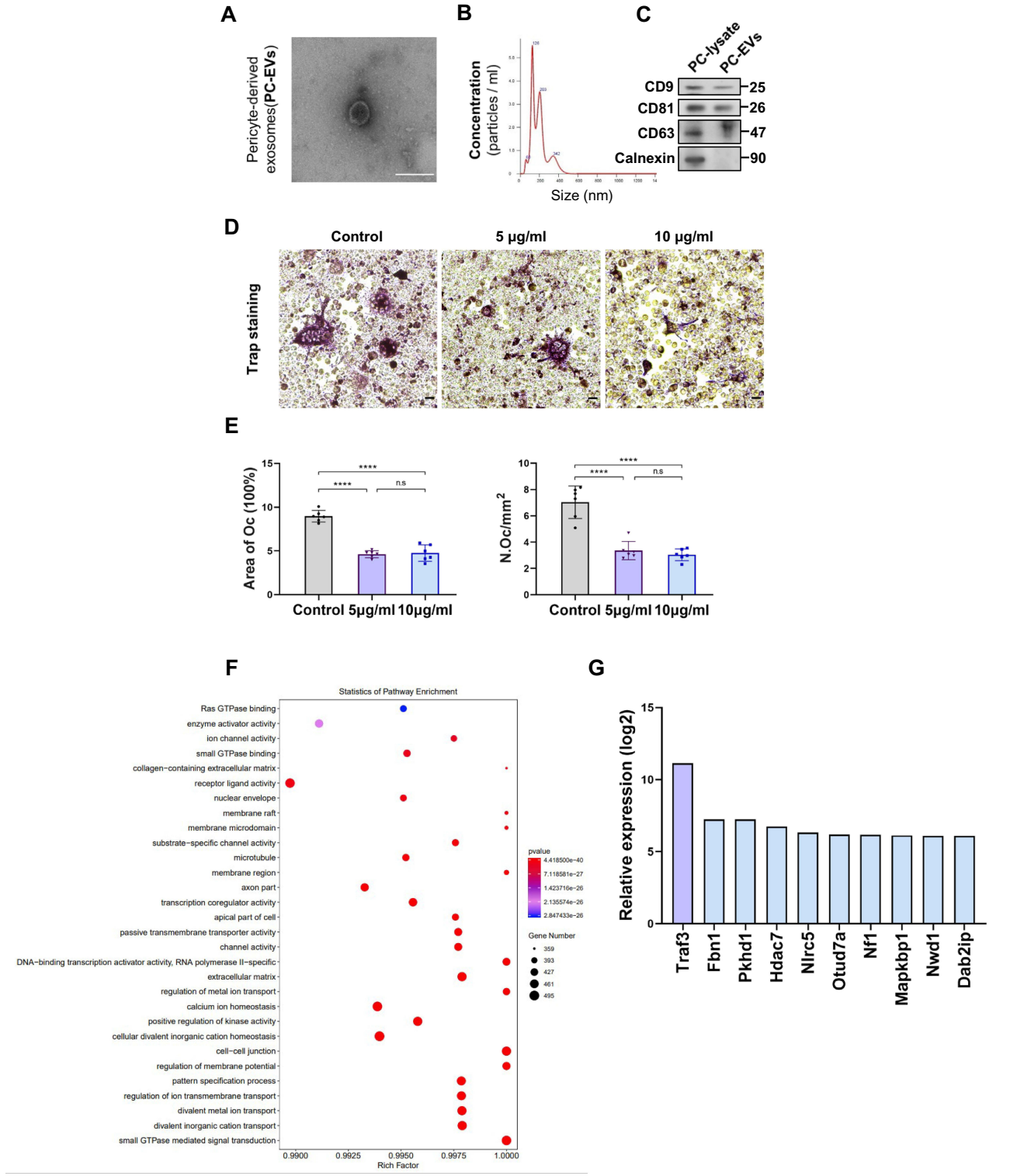

Figure 4 Traf3 in PC-EVs mediates the inhibition of osteoclast differentiation by pericytes (**A**) The images of PC-EVs under TEM. Bar, 100 μm. (**B**) NTA results of PC-EVs. (**C**) The characterization of PC-EVs by Western blotting. (**D**) Representative TRAP staining images of monocytes after 5 days of osteoclast differentiation. RAW264.7 cells were induced with a medium containing RANKL (100 ng/mL) and non-contact co-cultured with PC-EVs (5–10 μg/mL). Scale bar, 100 nm. (**E**) Quantification of osteoclast number (Oc.N) and area of osteoclast (area of oc) of monocytes after 5 days of osteoclast differentiation (n = 6). (**F**) GO analysis map of total RNA sequencing of PC-EVs. (**G**) The coding gene of osteoclast inhibitory protein. Data are presented as mean ± S.E.M. *P*-levels < 0.05 were considered statistically significant, as follows: ****$P < 0.0001$.

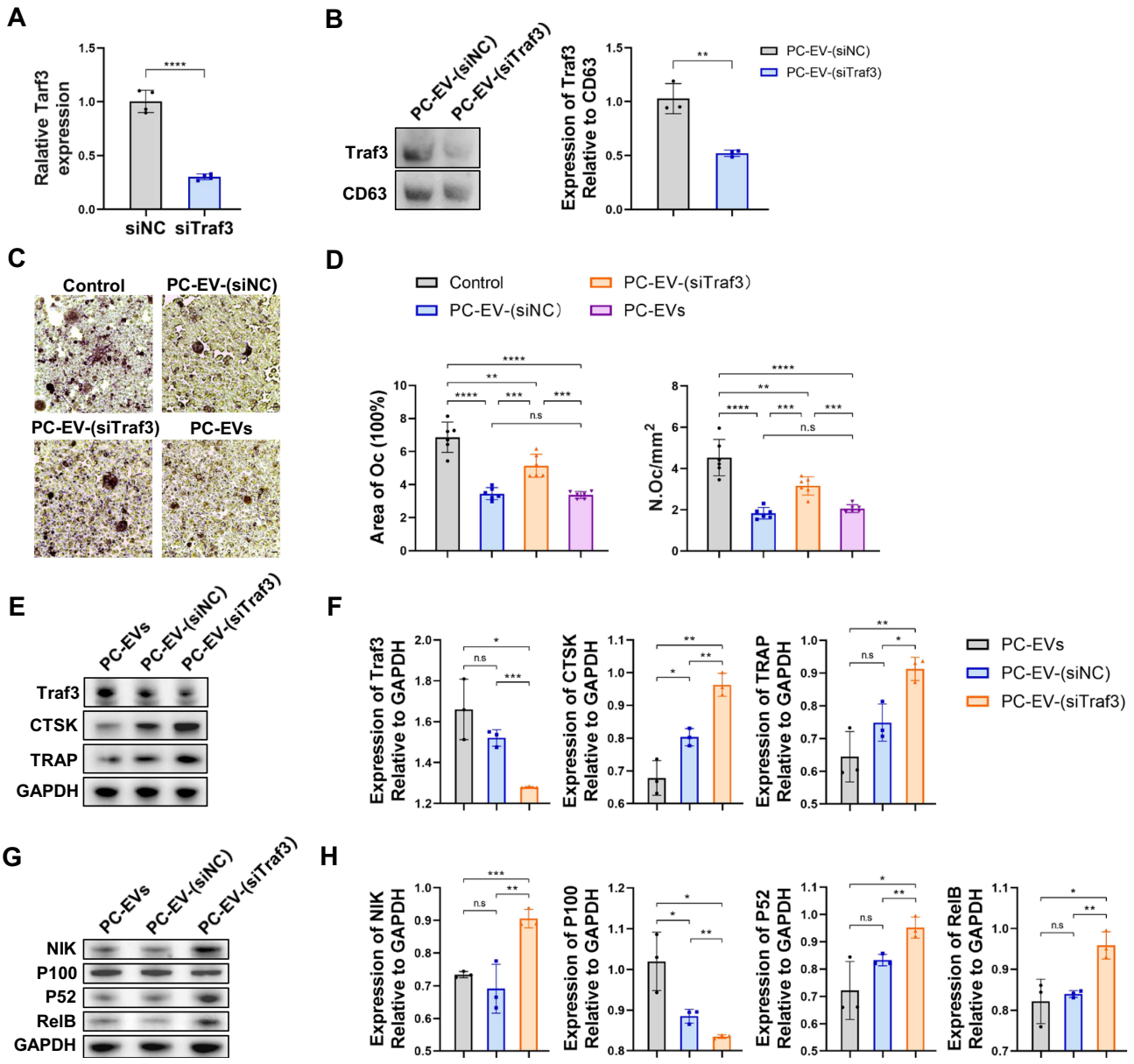

Figure 5 Traf3 inhibits osteoclast differentiation through the non-canonical NF-κB pathway (**A**) Relative mRNA expression of *Traf3* in vascular pericytes transfected with *Traf3* siRNA (n = 4). (**B**) Representative blots of exosome-derived TRAF3 and CD63, and quantification of the ratio of TRAF3/CD63 (n = 3). PC-EV-(siNC), exosomes generated from pericytes treated with *NC* siRNA. PC-EV-(siTraf3), exosomes generated from pericyte treated with *Traf3* siRNA. (**C**) Representative TRAP staining images of monocytes after 5 days of osteoclast differentiation. RAW264.7 cells were induced with a medium containing RANKL (100 ng/mL) and non-contact co-cultured with exosomes (5 μg/mL). Bar, 100μm (**D**) Quantification of osteoclast number (Oc.N) and area of osteoclast (area of oc) of monocytes after 5 days of osteoclast differentiation (n = 6). (**E**) Representative blots of TRAF3, TRAP, and CTSK of monocytes after 5 days of osteoclast differentiation. (**F**) Quantification of the ratio of TRAF3, TRAP, and CTSK/GAPDH in monocytes after 5 days of osteoclast differentiation (n = 3). (**G**) Representative blots of NIK, P100, P52, and RElB in monocytes after 5 days of osteoclast differentiation. (**H**) Quantification of the ratio of NIK, P100, P52, and RElB in monocytes after 5 days of osteoclast differentiation (n = 3). Data are presented as mean ± S.E. M. *P*-levels < 0.05 were considered statistically significant, as follows: **P* < 0.05; ***P* < 0.01; ****P* < 0.001; *****P* < 0.0001.

MMP-9.[25] Preosteoblasts secrete platelet-derived growth factor BB and recruit endothelial cells to promote angiogenesis.[26] Osteoblast-derived angiogenic factor Slit3 not only promotes vascular development but also inhibits osteoclast formation.[27] Reciprocally, vascular cells also affect bone formation to a certain extent. Endothelial cells promote osteoblast differentiation by producing interleukin-33,[28] and the endothelial cell-derived products, including endothelin, nitric oxide, and reactive oxygen species, are regulators of osteoclast function.[29]

However, the specific role of perivascular cells in bone metabolism has remained elusive. Our study reveals that low pericyte coverage is significantly correlated with increased bone resorption, and conditional deletion of pericytes in mice

activates bone resorption. These results indicate that pericytes negatively regulate osteoclast differentiation. To our understanding, this work is the first to shed light on the regulatory role of perivascular cells on osteoclasts, providing valuable evidence on their contribution to skeletal homeostasis.

Several preliminary studies have explored PC-EVs,[10,11,30,31] but their role in osteoclastogenesis remained unclear. In our study, RNA sequencing analysis in exosomes from bone perivascular cells revealed 2712 mRNAs related to bone formation, of which 815 were related to osteogenesis, 207 to cartilage, and up to 1479 to osteoclasts, highlighting the diversity of mRNA components and functions in these exosomes. Whether PC-EVs can regulate other bone properties needs a further investigation.

In our work, Traf3 in PC-EVs inhibited osteoclast differentiation by inhibiting the non-classical NF-κB pathway. TRAP and CTSK are osteoclast-specific genes, which are associated with the number of osteoclasts.[32–34] Studies have shown that Traf3 derived from PC-EVs inhibits osteoclast-specific gene expression. However, their inhibitory effect on osteoclastogenesis was not dose-dependent, with no significant difference observed between 5 μg/mL and 10 μg/mL PC-EVs.

In addition to the non-classical NF-κB pathway,[35,36] Traf3 also regulates apoptotic signaling in osteoclast precursor cells, influencing osteoclast formation.[37–39] It also prevents the degradation of β-catenin in mesenchymal progenitor cells, regulating osteoblast formation.[40] These findings suggest that Traf3's role in inhibiting osteoclast differentiation is connected to multiple signaling pathways.

The mechanism of exosome uptake is very complex and controversial, involving processes such as endocytosis, pinocytosis, phagocytosis, and membrane fusion.[41] However, the exact mechanism underlying the interaction between exosome-derived-Traf3 and RAW264.7 cells is still unknown.

Exosomes contain not only mRNA but also proteins, microRNAs (miRNAs), and long non-coding (lnc) RNAs.[42] Exosome-derived proteins induce osteoclast differentiation through stimulating the epidermal growth factor receptor (EGFR) pathway,[43] while exosome-derived miRNAs and lncRNAs have been shown to inhibit osteoclast differentiation.[44,45] Cytokines secreted by perivascular cells may play an essential role in maintaining the skeletal balance.[46] In addition, these substances may interact with each other.[44] Therefore, additional investigations are warranted to clarify the negative regulatory effect of exosome-derived proteins, lncRNAs, or miRNAs and their interactions from perivascular cells on osteoclasts, and the inhibitory effect of perivascular cell-derived cytokines on osteoclast differentiation.

Although we may still require additional investigation in certain areas, this study offers a novel concept of pericytes closely associated with the induction of osteoclast activity in various bone disorders, such as osteoarthritis and osteoporosis.[47,48] Patients with osteoporosis are characterized by enhanced osteoclast activity.[48] In our study, pericytes have been shown to suppress osteoclasts, and the inhibitory signal produced by pericytes may offer a novel approach to treating osteoporosis. Furthermore, since the development of H-type blood vessels in osteoarthritis is intimately related to the activation of osteoclasts,[49] pericytes may also be crucial in vascular remodeling. Future research on the potential therapeutic benefit of pericytes in disorders affecting the skeletal system is therefore essential.

Conclusion

In summary, our work demonstrates that pericytes regulate osteoclasts and inhibit osteoclastogenesis through exosomes. PC-EVs negatively regulates osteoclastogenesis through Traf3 by inhibiting the non-classical NF-κB pathway. These approaches hold promise as potential therapeutic strategies for conditions characterized by bone resorption.

Data Sharing Statement

The data supporting the findings of this study are available from the corresponding author upon reasonable request.

Ethics Approval

All animal experiments received the approval of the Experimental Animal Ethics Committee of Jinan University (Approval No.: IACUC-20230322-03; Date: 2023-03-22). And all experiments involving animals followed the national

standards of the People's Republic of China (Laboratory animal—Guideline for ethical review of animal welfare [GB/T 35892–2018].

Funding

This work was generously supported by the National Natural Science Foundation of China (82201001), the Natural Science Foundation Projects of Guangdong (2021A1515010882), the Science and Technology Projects in Guangzhou (202102010040, 202201010315 and 2023A03J1030), and the Clinical Frontier Technology Program of the First Affiliated Hospital of Jinan University, China (JNU1AF-CFTP-2022-a01210).

Disclosure

The authors declare no conflicts of interest in this work.

References

1. Teichert M, Milde L, Holm A, et al. Pericyte-expressed Tie2 controls angiogenesis and vessel maturation. *Nat Commun*. 2017;8(1):16106. doi:10.1038/ncomms16106
2. Armulik A, Genové G, Betsholtz C. Pericytes: developmental, physiological, and pathological perspectives, problems, and promises. *Dev Cell*. 2011;21(2):193–215. doi:10.1016/j.devcel.2011.07.001
3. Chim SM, Tickner J, Chow ST, et al. Angiogenic factors in bone local environment. *Cytokine Growth Factor Rev*. 2013;24(3):297–310. doi:10.1016/j.cytogfr.2013.03.008
4. Ramasamy SK, Kusumbe AP, Wang L, Adams RH. Endothelial notch activity promotes angiogenesis and osteogenesis in bone. *Nature*. 2014;507(7492):376–380. doi:10.1038/nature13146
5. Negri S, Wang Y, Sono T, et al. Human perivascular stem cells prevent bone graft resorption in osteoporotic contexts by inhibiting osteoclast formation. *Stem Cells Transl Med*. 2020;9(12):1617–1630. doi:10.1002/sctm.20-0152
6. Davaine JM, Quillard T, Brion R, et al. Osteoprotegerin, pericytes and bone-like vascular calcification are associated with carotid plaque stability. *PLoS One*. 2014;9(9):e107642. doi:10.1371/journal.pone.0107642
7. Davaine JM, Quillard T, Chatelais M, et al. Bone like arterial calcification in femoral atherosclerotic lesions: prevalence and role of osteoprotegerin and pericytes. *Eur J Vasc Endovasc Surg*. 2016;51(2):259–267. doi:10.1016/j.ejvs.2015.10.004
8. Elsharkasy OM, Nordin JZ, Hagey DW, et al. Extracellular vesicles as drug delivery systems: why and how? *Adv Drug Deliv Rev*. 2020;159:332–343. doi:10.1016/j.addr.2020.04.004
9. Kalluri R, LeBleu VS. The biology, function, and biomedical applications of exosomes. *Science*. 2020;367(6478). doi:10.1126/science.aau6977
10. Huang M, Chen M, Qi M, et al. Perivascular cell-derived extracellular vesicles stimulate colorectal cancer revascularization after withdrawal of antiangiogenic drugs. *J Extracell Vesicles*. 2021;10(7):e12096. doi:10.1002/jev2.12096
11. Liu C, Ge HM, Liu BH, et al. Targeting pericyte-endothelial cell crosstalk by circular RNA-cPWWP2A inhibition aggravates diabetes-induced microvascular dysfunction. *Proc Natl Acad Sci U S A*. 2019;116(15):7455–7464. doi:10.1073/pnas.1814874116
12. Song H, Li X, Zhao Z, et al. Reversal of osteoporotic activity by endothelial cell-secreted bone targeting and biocompatible exosomes. *Nano Lett*. 2019;19(5):3040–3048. doi:10.1021/acs.nanolett.9b00287
13. Cooke VG, LeBleu VS, Keskin D, et al. Pericyte depletion results in hypoxia-associated epithelial-to-mesenchymal transition and metastasis mediated by met signaling pathway. *Cancer Cell*. 2012;21(1):66–81. doi:10.1016/j.ccr.2011.11.024
14. Wilson CL, Stephenson SE, Higuero JP, Feghali-Bostwick C, Hung CF, Schnapp LM. Characterization of human PDGFR-β-positive pericytes from IPF and non-IPF lungs. *Am J Physiol-Lung Cel Molecul Physiol*. 2018;315(6):L991–L1002. doi:10.1152/ajplung.00289.2018
15. Li D, Liu J, Guo B, et al. Osteoclast-derived exosomal miR-214-3p inhibits osteoblastic bone formation. *Nat Commun*. 2016;7(1):10872. doi:10.1038/ncomms10872
16. Smith ZJ, Lee C, Rojalin T, et al. Single exosome study reveals subpopulations distributed among cell lines with variability related to membrane content. *J Extracell Vesicles*. 2015;4(1):28533. doi:10.3402/jev.v4.28533
17. Zeng XZ, He LG, Wang S, et al. Aconine inhibits RANKL-induced osteoclast differentiation in RAW264.7 cells by suppressing NF-κB and NFATc1 activation and DC-STAMP expression. *Acta Pharmacol Sin*. 2016;37(2):255–263. doi:10.1038/aps.2015.85
18. Ozerdem U, Monosov E, Stallcup WB. NG2 proteoglycan expression by pericytes in pathological microvasculature. *Microvascu Res*. 2002;63(1):129–134. doi:10.1006/mvre.2001.2376
19. Murfee WL, Skalak TC, Peirce SM. Differential arterial/venous expression of NG2 proteoglycan in perivascular cells along microvessels: identifying a venule-specific phenotype. *Microcircul*. 2005;12(2):151–160. doi:10.1080/10739680590904955
20. Liu C, Shao ZM, Zhang L, et al. Human endomucin is an endothelial marker. *Biochem Biophys Res Commun*. 2001;288(1):129–136. doi:10.1006/bbrc.2001.5737
21. He JQ, Saha SK, Kang JR, Zarnegar B, Cheng G. Specificity of TRAF3 in its negative regulation of the noncanonical NF-kappa B pathway. *J Biol Chem*. 2007;282(6):3688–3694. doi:10.1074/jbc.M610271200
22. He JQ, Zarnegar B, Oganesyan G, et al. Rescue of TRAF3-null mice by p100 NF-κB deficiency. *J Exp Med*. 2006;203(11):2413–2418. doi:10.1084/jem.20061166
23. Armulik A, Abramsson A, Betsholtz C. Endothelial/pericyte interactions. *Circ Res*. 2005;97(6):512–523. doi:10.1161/01.RES.0000182903.16652.d7
24. Shepro D, Morel NM. Pericyte physiology. *FASEB j*. 1993;7(11):1031–1038. doi:10.1096/fasebj.7.11.8370472
25. Cackowski FC, Anderson JL, Patrene KD, et al. Osteoclasts are important for bone angiogenesis. *Blood*. 2010;115(1):140–149. doi:10.1182/blood-2009-08-237628

26. Xie H, Cui Z, Wang L, et al. PDGF-BB secreted by preosteoclasts induces angiogenesis during coupling with osteogenesis. *Nat Med*. 2014;20(11):1270–1278. doi:10.1038/nm.3668
27. Xu R, Yallowitz A, Qin A, et al. Targeting skeletal endothelium to ameliorate bone loss. *Nat Med*. 2018;24(6):823–833. doi:10.1038/s41591-018-0020-z
28. Kenswil KJG, Jaramillo AC, Ping Z, et al. Characterization of endothelial cells associated with hematopoietic niche formation in humans identifies il-33 as an anabolic factor. *Cell Rep*. 2018;22(3):666–678. doi:10.1016/j.celrep.2017.12.070
29. Zaidi M, Alam AS, Bax BE, et al. Role of the endothelial cell in osteoclast control: new perspectives. *Bone*. 1993;14(2):97–102. doi:10.1016/8756-3282(93)90234-2
30. Yuan X, Wu Q, Wang P, et al. Exosomes derived from pericytes improve microcirculation and protect blood-spinal cord barrier after spinal cord injury in mice. *Front Neurosci*. 2019;13:319. doi:10.3389/fnins.2019.00319
31. Ye L, Guo H, Wang Y, et al. Exosomal circEhmt1 released from hypoxia-pretreated pericytes regulates high glucose-induced microvascular dysfunction via the nfia/nlrp3 pathway. *Oxid Med Cell Longev*. 2021;2021:8833098. doi:10.1155/2021/8833098
32. Boyle WJ, Simonet WS, Lacey DL. Osteoclast differentiation and activation. *Nature*. 2003;423(6937):337–342. doi:10.1038/nature01658
33. Lacey DL, Timms E, Tan HL, et al. Osteoprotegerin ligand is a cytokine that regulates osteoclast differentiation and activation. *Cell*. 1998;93(2):165–176. doi:10.1016/S0092-8674(00)81569-X
34. Suzuki N, Yoshimura Y, Deyama Y, Suzuki K, Kitagawa Y. Mechanical stress directly suppresses osteoclast differentiation in RAW264.7 cells. *Int J Mol Med*. 2008;21(3):291–296.
35. Boyce BF, Li J, Xing L, Yao Z. Bone remodeling and the role of traf3 in osteoclastic bone resorption. *Front Immunol*. 2018;9:2263. doi:10.3389/fimmu.2018.02263
36. Xiu Y, Xu H, Zhao C, et al. Chloroquine reduces osteoclastogenesis in murine osteoporosis by preventing TRAF3 degradation. *J Clin Invest*. 2014;124(1):297–310. doi:10.1172/JCI66947
37. Xue Y, Liang Z, Fu X, Wang T, Xie Q, Ke D. IL-17A modulates osteoclast precursors' apoptosis through autophagy-TRAF3 signaling during osteoclastogenesis. *Biochem Biophys Res Commun*. 2019;508(4):1088–1092. doi:10.1016/j.bbrc.2018.12.029
38. Xu S, Li S, Liu X, et al. Rictor is a novel regulator of TRAF6/TRAF3 in osteoclasts. *J Bone Miner Res*. 2021;36(10):2053–2064. doi:10.1002/jbmr.4398
39. Ke D, Zhu Y, Zheng W, Fu X, Chen J, Han J. Autophagy mediated by JNK1 resists apoptosis through TRAF3 degradation in osteoclastogenesis. *Biochimie*. 2019;167:217–227. doi:10.1016/j.biochi.2019.10.008
40. Li J, Ayoub A, Xiu Y, et al. TGFβ-induced degradation of TRAF3 in mesenchymal progenitor cells causes age-related osteoporosis. *Nat Commun*. 2019;10(1):2795. doi:10.1038/s41467-019-10677-0
41. Mulcahy LA, Pink RC, Carter DR. Routes and mechanisms of extracellular vesicle uptake. *J Extracell Vesicles*. 2014;3(1):24641.
42. Pegtel DM, Gould SJ. Exosomes. *Annu Rev Biochem*. 2019;88(1):487–514. doi:10.1146/annurev-biochem-013118-111902
43. Taverna S, Pucci M, Giallombardo M, et al. Amphiregulin contained in NSCLC-exosomes induces osteoclast differentiation through the activation of EGFR pathway. *Sci Rep*. 2017;7(1):3170. doi:10.1038/s41598-017-03460-y
44. Zhang Y, Xie RL, Croce CM, et al. A program of microRNAs controls osteogenic lineage progression by targeting transcription factor Runx2. *Proc Natl Acad Sci U S A*. 2011;108(24):9863–9868. doi:10.1073/pnas.1018493108
45. Yang Z, Liu X, Zhao F, et al. Bioactive glass nanoparticles inhibit osteoclast differentiation and osteoporotic bone loss by activating lncRNA NRON expression in the extracellular vesicles derived from bone marrow mesenchymal stem cells. *Biomaterials*. 2022;283:121438. doi:10.1016/j.biomaterials.2022.121438
46. Zhu S, Bennett S, Kuek V, et al. Endothelial cells produce angiocrine factors to regulate bone and cartilage via versatile mechanisms. *Theranostics*. 2020;10(13):5957–5965. doi:10.7150/thno.45422
47. Zhang H, Wang L, Cui J, et al. Maintaining hypoxia environment of subchondral bone alleviates osteoarthritis progression. *Sci Adv*. 2023;9(14):eabo7868. doi:10.1126/sciadv.abo7868
48. Rachner TD, Khosla S, Hofbauer LC. Osteoporosis: now and the future. *Lancet*. 2011;377(9773):1276–1287. doi:10.1016/S0140-6736(10)62349-5
49. Hu Y, Chen X, Wang S, Jing Y, Su J. Subchondral bone microenvironment in osteoarthritis and pain. *Bone Res*. 2021;9(1):20. doi:10.1038/s41413-021-00147-z